The Involvement of PPARγ In Anti-Inflammatory Activity of N-Stearoylethanolamide

Halyna Kosiakova
Palladin Institute of Biochemistry National Academy of Sciences of Ukraine: Institut biohimii imeni O V Palladina Nacional'na akademia nauk Ukraini https://orcid.org/0000-0002-1214-2044

Andrii Berdyshev (a3318279@outlook.com)
O V Palladin Institute of Biochemistry National Academy of Sciences of Ukraine
https://orcid.org/0000-0002-4690-1184

Victor Dosenko
Bogomoletz Institute of Physiology National Academy of Sciences of Ukraine: Institut Fiziologii imeni O O Bogomolca Nacional'na akademia nauk Ukraini

Tetyana Drevytska
Bogomoletz Institute of Physiology National Academy of Sciences of Ukraine: Institut Fiziologii imeni O O Bogomolca Nacional'na akademia nauk Ukraini

Oleksandra Herasymenko
Palladin Institute of Biochemistry National Academy of Sciences of Ukraine: Institut biohimii imeni O V Palladina Nacional'na akademia nauk Ukraini

Nadiya Hula
Palladin Institute of Biochemistry National Academy of Sciences of Ukraine: Institut biohimii imeni O V Palladina Nacional'na akademia nauk Ukraini

Research Article

Keywords: N-stearoylethanolamide, PPAR, NF-kB, IL-1β, inflammation

Posted Date: July 8th, 2021

DOI: https://doi.org/10.21203/rs.3.rs-636781/v1

Abstract

N-stearoylethanolamide (NSE)– a cannabinoid-like compound with wide range of biological activity. Anti-inflammatory properties of NSE have been indicated on different animal models of pathological conditions. However, the molecular mechanisms of anti-inflammatory action of NSE remain unclear. In the current study, the involvement of PPARγ in the NF-kB -dependent anti-inflammatory action of NSE was evaluated using different methodological approach. First method - molecular modeling, evaluated the possibility of NSE to bind with PPAR. Then, in ex vivo experiment, using selective synthetic agonist of PPARα/γ LY-171883 and selective antagonist of PPARγ - GW9662, the role of PPARα /PPARγ in the NSE's effect on nuclear NF-kB translocation was examined in LPS-activated rat peritoneal macrophages. Finally, the NSE action on the mRNA level of several PPARγ- dependent genes was studied in liver of insulin-resistant rats.

The molecular docking results showed that NSE could bind to PPARγ and compete for the binding with antagonist GW9662 and agonist LY171883 in the active site of PPARγ. It also has been found that NSE prevented the LPS-induced NF-kB translocation into the nuclei of rat peritoneal macrophages during pre-treatment with NSE before LPS application. When NSE was added before GW9662 and LPS treatment, the level of NF-kB translocation and IL-1β content reduced to control cells' levels. These data confirmed a competitive binding of NSE with GW9662 for the ligand-binding domen of PPARγ. In addition, NSE administration to insulin resistant rats changed the mRNA expression of several PPARγ target gens, including FATP1 and IL1-ra.

Introduction

N-stearoylethanolamide (NSE) is a member of endogenous class of lipid signaling molecules - N-acylethanolamides (NAEs). NAEs are produced "on demand" from their precursors N-acylated phosphatidylethanolamide (NAPE) in response to tissue injury and stress to restore homeostatic balance and prevent further damage [1]. NAEs are the derivatives of ethanolamide and fatty acids with different length and saturation of acyl chain that determinate their biological activity. Some of the NAEs (anandamide) belong to endocannabinoid system and mainly exert their biological action by activating cannabinoid receptors (CB) [2]. NAEs with saturated chains (N-palmitoylethanolamide and N-stearoylethanolamide) are CB inactive, however, they show cannabimimetic / cannabinoid-like properties [3]. Various biological and pharmacological effects of NSE have been reported under different pathological conditions. NSE has been shown to protect cells from oxidative stress [4], exhibiting membranoprotective [5], neuroprotective [6] and adaptogenic properties [7], as well as anorexic [8] and anti-inflammatory action [9].

In our previously studies we have reported that NSE normalizes liver and pancreas lipid composition, increases insulin sensitivity and restores the ratio of LDL / HDL in blood plasma of rats with obesity-induced insulin resistance (IR) [10].

Over the past 2 decades, different researches revealed that obesity and insulin resistance are associated with chronic low-grade inflammation.

It is widely confirmed that NF-kB is one of the major transcription factors responsible for adaptive cellular responses and inflammation. NF-kB affects various genes involved in the immune, acute-phase, inflammatory response of the body. Such as IL-10, TNFα, IL-2, IL-6, IL-12, IL-8 and other chemokines, inducible enzymes (iNOS, Cox-2), adhesion molecules (ICAM-1, VCAM-1, E) selectin), the major histocompatibility complex (MHC-I, MHC-P), complementary proteins (B, C3, C4), contiguous cell cycle factors (p53, cyclin D1, etc.), inhibitors and activators of apoptosis (IAP1, c-IAP2, FasL, Bcl-2, TRAF-TRAF-2, etc.) [11-14]. Earlier, we have reported that NSE exert the anti-inflammatory action by inhibiting NF-kB translocation into the nuclei of the LPS-activated rat peritoneal macrophages [15].

It is known that PPARγ capable of affecting the transcriptional activity of NF-κB and thus play a key role in the regulation of inflammation and dyslipidemia [16, 17].

We assumed that current NSE action could be implemented by interaction with PPARγ. Therefore, the aim of this study was to reveal the involvement of PPARγ in the mechanisms of anti-inflammatory action of NSE.

Materials And Methods

2.1. Reagents

NSE was synthesized in the Department of Lipid Biochemistry at Palladin Institute of Biochemistry as described previously [18,19]. Primers were purchased at Metabion (Litva).

2.2. Molecular modeling

The interaction of N-stearoylethanolamide, LY171883 (PPARα / γ agonist), GW6471 (synthetic PPARα antagonist), and GW9662 (synthetic PPARγ antagonist) with PPARα / γ subtypes was performed by molecular docking. Spatial structures of α- (1kkq) ligand-binding domain and PPAR subtypes of γ- (3b0r) were used from the online resource RCSB Protein DataBank, N-stearoylethanolamide, GW6471 and GW9662 from ChemSpider. The spatial structures of PPAR ligand-binding domain were prepared for docking in the AutoDockTools 1.5.6 program. The same program was used for the visualization of interaction between investigated ligands and amino acid residues of the PPARα / γ molecule. The lowest level of free binding energy between the ligand and macromolecule corresponded to the positioning of the ligand in the ligand-binding domain of the receptor that was calculated using the program AutoDock Vina 1.1.2.

2.3. Peritoneal macrophages isolation procedure

Male Sprague-Dawley rats (220 ± 20 g) were used in the study. All procedures were conducted in accordance with the rules of Commission on Bioethics of Institute of Biochemistry, National Academy of Science and with “General ethics principles on experiments with animals” of the 1st National Congress on Bioethics (Kyiv, 2001). Rat resident peritoneal macrophages were collected by lavaging rat peritoneal cavity with RPMI-1640 and cultivated directly on the glass cover-slips in a 35 mm dish (1.6×10^6 cell in each sample) during 60 min with 10 μL lipopolysaccharide (LPS) (from Escherichia coli 0127:B8, Sigma-Aldrich) solution (1 mg/mL PBS). 15 min before LPS stimulation the water suspension of NSE (10^{-7}M) and/or selective agonist of PPAR-α/γ LY-171,883 (Sigma-Aldrich, cat. #L5408) 125 μM, selective antagonist of PPARγ GW9662 (Sigma-Aldrich, cat. #M6191) 1.25 μM were added to the medium.

2.4. Immunofluorescence confocal microscopy

The NF-κB activation was determined by immunofluorescence assay, evaluating the nuclear translocation of NF-κB p-65 subunits. Cells were fixed with 3.5 % paraformaldehyde in PBS for 10 min at room temperature and permeabilized with 0.2% Triton X-100 (in PBS) for 5 min. To investigate the cellular localization of NF-κB, cells were treated with a rabbit polyclonal antibody against NF-κB p65 (Abcam, cat. #ab16502) diluted at 1:600 in 1% albumin on PBS for 1.5 h. After extensive washing with PBS, cells were further incubated with a goat secondary FITC-conjugated donkey anti-rabbit IgG antibody (Abcam, cat. #ab6717) diluted at 1:500 in 0.1% albumin on PBS for 1h at a room temperature. Nuclei were stained with 0.5 g/mL of DAPI (Sigma-Aldrich, cat. #D9542), and then were analyzed with Zeiss LSM 510 Meta confocal microscope. Randomly, 30–150 cells from each confocal image (1024 × 1024 pixels) were counted with independently developed software based on ImageEn component suite (Xequte Software, New Zealand) that calculated the percentage of green pixels in the nucleus zone. The percentage of FITC particles (p65 subunit of NF- κB) was equal to green pixels.

2.5. Cytokine level measurement

The IL-1β level in supernatants of rat peritoneal macrophages was measured using ELISA kit (eBioscience, Austria, cat. #BMS630).

2.6. Animal model.

The study was carried out on male Sprague-Dawley rats (188 ± 38 g). All procedures were conducted in accordance with the rules of Commission on Bioethics of Institute of Biochemistry, National Academy of Science and with “General ethics principles on experiments with animals” of the 1st National Congress on Bioethics (Kyiv, 2001). Rats were housed in standard cages with free access to food and water. Obesity-induced insulin resistant IR in rats was attained by prolonged high-fat diet (58% fat: 23% proteins:10 % carbohydrates) as described earlier [10]. The amount of lipids in the diet was increased by addition of lard to the pellet chow. The high-fat diet (HFD) contained 55% of saturated (24% palmitic and 28% stearic acid) and 45% of unsaturated fatty acid. Control rats during the experiment were on normal pellet diet (4% fat: 23% proteins: 65% carbohydrates) with saturated/unsaturated fatty acid ratio 38%/62%, respectively. Six months after HFD period, the oral glucose tolerance test was conducted [10]. Obtained results showed

that after glucose administration (1 mL of 50% glucose solution) to HFD rats, blood glucose level was 8.5 mM within 90 min (in controls –5.1mM), and more than 5mM within 150 min (in controls –decreased to normal levels – 3.8 mM). Rats that showed impaired glucose tolerance were selected and divided into 2 groups: IR and IR + NSE. Rats from IR+NSE group were treated with water suspension of NSE, per os, at a dose of 50 mg per kg of body weight, during 14 days.

Control rats with normal glucose tolerance were further subdivided into control (n =10) and NSE (n= 7) groups. Animals in NSE and IR + NSE groups were orally received the water suspension of NSE for 2 weeks at the dose of 50 mg/kg of body weight. This particular dose of NSE has been chosen as an optimal reacting dose for the research. Schmid H. H et al. earlier reported the exact concentration of NSE found during the experiment of dog coronary artery occlusion [20]. The establishment of IR was confirmed based on the results of fasting plasma insulin levels (measured by ELISA kit, DRG Germany) and HOMA-IR (homeostatic model assessment – insulin resistance) value, calculated by fasting insulin (nM) × Fasting glucose (mM)/22.5.

At the end of the experiment, the rats were scarified under Nembutal anesthesia (50 mg/kg body weight). The liver was immediately removed and frozen at-80°C until further analysis.

2.7. RT-PCR analysis

RT-PCR analysis was used for evaluating the relative level of PPAR-target genes (fatty acid transporter protein (FATP) gene and interleukin-1 receptor antagonist (IL-1ra) gene) mRNA in rat liver.

RNA was isolated from rat liver tissue using TRI Reagent (Sigma-Aldrich) according to the manufacturer's instructions. The concentration of the isolated RNA was determined using a NanoDrop 1000 spectrophotometer (Thermo Scientific, USA). Reverse transcription was performed using First Strand cDNA Synthesis Kit (k1612, Thermo Scientific™, USA) and 1.5 micrograms of total RNA, as well as hexamer primer. Obtained complementary DNA was used as a template for gene-specific PCR amplification. To evaluate of the mRNA expression, primers of the following sequence were used for FATP1: forward 5’- GAC TTC TCA CTC TGA GCC TGG T-3’ , and reverse 5’-GTG TGC ATA GTG GGT TGT AGG A-3’; for IL1RN: forward 5’-CAA GAA CAA AGA AGA AGA CAA GCG-3’, and reverse 5’-GCA AGT GAT TCG AAG CTG GTG-3'. Expression of genes was analyzed against the expression of the β-actin gene as an endogenous control, the primers of which had the following sequences: β-Actin: forward 5’-CTTAGAGGGACAAGTGGCG-3’ and reverse 5’-GGACATCTAAGGGCATCACA-3’.

PCR amplification of genes was performed in 10 µl of SYBR™ Green PCR Master Mix (Catalog number: 4309155, ThermoFisher, USA) containing 40 pmoles of each primer. The volume was brought to 20 µl of deionized water. The amplification was performed in the "7500 Fast Real-Time PCR System" thermocycler. The amplification program began with the preliminary activation of AmpliTag Gold® DNA polymerase for 10 min at t = 95.0 ° C and included 45 cycles each consisting of denaturation at t = 95.0 ° C (19 s), primer attachment and elongation at t = 58.0 ° C (1 min). To control specificity, a dissociation step was added - a consistent increase in temperature from 58.0 to 95.0 ° C, with the recording of a

decrease in the fluorescence intensity of double-stranded DNA complexes with SYBR Green. The relative level of gene expression was determined using a commonly used technique (expression level = 2-ΔCt, where Ct is the threshold amplification cycle). We calculated the expression of the target gene relative to the housekeeping gene as the difference between the threshold values of both genes.

2.Statistical Analysis

The data presented as mean values ± standard errors of the means (SEM) from different studied groups were compared by one-way analysis of variance (ANOVA). The correlation coefficient (r) was calculated using function CORREL from Microsoft EXCEL 365. The statistical significance was determined at the level of $p<0.05$.

Results

3.1 Molecular modeling of NSE, GW9662 and LY171883 binding to PPARγ

The results of the molecular docking have shown that all studied ligands bind to the same region of the PPARγ ligand-binding domain in the position corresponding to the lowest binding energy (fig. 1). Thus, they all can compete for binding sites in the PPAR γ active center.

The detected amino acid residues involved in the interaction of all investigated ligands in a position with a minimum binding energy with the PPAR γ molecule are shown in Table 1.

Table 1. The individual docking data of GW9662, NSE, and LY171883 to the ligand-binding domain of PPARγ

PPAR-active compounds	GW9662	NSE	LY 171883
Gibbs free energy of binding (kcal/mol)	-7,9	-6,6	-7,7
Amino acid residues involved in the binding		Leu228	
		Ile281	
			Gly284
			Cys285
	Arg288	Arg288	Arg288
			Ser289
	Ala292		
	Ile326	Ile326	
	Met329		
	Leu330	Leu330	Leu330
			Ile341
			Ser342
		Met364	
		Phe380	

The individual docking data of NSE, GW9662 and LY171883 showed that all studied compounds have close binding energy (Gibbs free energy) and common sites (amino acid residues) in the active center of the PPARγ molecule (3b0r).

3.2 Effects of GW6992, LY171883 and NSE on the NF-kB translocation in the nucleus of rat activated peritoneal macrophages

We found that NSE administration to the normal macrophages did not affect the NF-kB translocation to the nuclei (Fig.2. bar chart. 2. Typical confocal image of the peritoneal macrophages slides has shown in supplement 1). The LPS stimulation of isolated rat peritoneal macrophages exerted the increase in the percentage of FITC -labeled particles in the nucleus of macrophages compare to control untreated cells (Fig.2, bar chart 3). These findings indicated an increase in the number of NF-κB dimer molecules in the nucleus of peritoneal macrophages after LPS treatment. It was accompanied by enhanced content of IL-1β in the culture supernatant (Fig.3, bar chart 3). The pre-incubation of macrophages with NSE before the LPS treatment resulted in decreased amount of FITC-IgG in nuclei compare to LPS-treated cells (Fig. 2, bar chart 4). While the IL-1β content was at the same level as in control cells (Fig.6, bar chart 4). The incubation of macrophages with a selective synthetic agonist of PPARα/γ LY-171,883 before the LPS stimulation resulted in significant decrease of nucleus content of FITC-IgG compared to both control and

LPS-activated macrophages. (Fig. 2, bar chart 5), followed by significant reduction of IL-1β level (Fig.3, bar chart 5). Meanwhile, enhanced number of FITC-IgG was detected in the nucleus of peritoneal macrophages (Fig.2, bar chart 6) as well as elevated content of IL-1β (Fig.3, bar chart 6) in LPS stimulated macrophages that were pre-incubated with selective PPARγ antagonist GW9662. The similar data was obtained during initial cell incubation with GW9662 and after that with NSE before LPS-activation (Fig. 2, bar chart 7; Fig. 3, bar chart 7). However, initial incubation of macrophages with NSE and after that with GW9662 before LPS treatment, prevented the increase of FITC-IgG particles in the nucleus (Fig. 2, bar chart 8) and IL-1β content in the culture supernatant (Fig. 3, bar chart 8).

Summarizing, there was a positive correlation between the content of IL-1β in the culture supernatant of peritoneal macrophages and the amount of FITC-IgG in their nucleus ($r = 0.87$; $P < 0.001$).

3.3 Effect of GW6471, LY171883 and NSE on the NF-kB translocation in the nucleus of activated rat peritoneal macrophages

We did not observe any increase in the number of FITC-IgG particles in nuclei of peritoneal macrophages that were treated with selective PPARα antagonist GW6471 before LPS stimulation (Fig.4, bar chart 6). Typical confocal images of the peritoneal macrophages slides presented in supplement 1. This finding indicated that PPARα was less involved in the anti-inflammatory action compared to PPARγ. When NSE was added in both cases (before and after GW6471) before LPS- stimulation, the FITC-IgG number in the nucleus of peritoneal macrophages was at the control (untreated cells) level (Fig.4, bar chart 7,8).

In rats with obesity –induced IR a slight increase of FATP mRNA expression was detected in liver. Our results demonstrated that liver level of FATP mRNA expression in IR rats treated with NSE was 2- fold higher than in control rats (Fig. 8). Meanwhile, NSE administration to control rats did not cause any changes in the liver level of FATP mRNA expression.

Furthermore, detection of mRNA Il-1 ra expression in the liver of NSE-treated IR rats showed 2.2 –fold higher level compared to control rats. The administration of NSE to control rats caused a decrease of mRNA Il-1 ra liver expression. The level of mRNA Il-1 ra expression in liver of IR rats was not significantly higher in a relation to control rats.

Discussion

The involvement of endocannabinoid system in the regulation of inflammatory processes in various pathological conditions is beyond doubt and has been well studied. It worth to note that the endocannabinoid system includes compounds with different chemical structure that can activate cannabinoid receptors or exert cannabinoid-like properties via different pathways. Some of endocannabinoids have shown anti-inflammatory effects that may be realized with participation of cannabinoid receptors or by using other mechanisms. Primarily, due to direct action on participating immune cells, or by changing the local endocannabinoid concentrations that followed by anti-inflammatory actions. It was confirmed that endocannabinoid anandamide exerts anti-inflammatory

action via cannabinoid receptor–independent pathway by inhibiting NF-κB activation [21]. N-palmitoylethanolamide (NPE) is an endocannabionoid-like compound that is presented in nature, numerous foods, and is endogenously produced by our body, acted as a balancer of inflammatory processes. NPE activated the PPARα and in this way eliminated the anti-inflammatory activity [22]. NSE is a congener of NPE. Little is known about the NSE anti-inflammatory activity. Previously, on the different models of pathological conditions we have shown that NSE decreased the production and content of inflammatory cytokines (IL-1β, TNF-α) [15]. Further studies reported that particular NSE effect was associated with the inhibition of nuclear NF-κB translocation in LPS- activated rat peritoneal macrophages [23]. It is known that LPS-induced inflammatory response could be inhibited by the activation of either PPAR-γ or LXRα [24, 25].

The results of this study indicated the possible involvement of PPARγ in the mediation of NSE anti-inflammatory action. With the method of molecular modeling, we showed that NSE could bind to PPARγ and compete for the binding with antagonist GW9662 and agonist LY171883 in the active site of the PPARγ. In *ex vivo* experiment we used selective synthetic agonist of PPARα/γ LY-171883 and selective antagonist of PPARγ GW9662 to study the role of PPARα /PPARγ in the NSE's effect on nuclear NF-kB translocation in LPS-activated rat peritoneal macrophages. In addition, the action of NSE on the mRNA level of several PPARγ- dependent genes (FATP1 and IL1RN) has been studied in liver of IR rats.

The incubation of peritoneal macrophages with PPAR α/γ selective agonist LY- 171.883 before LPS activation resulted in inhibition of nuclear NF-kB translocation followed by a decrease of IL-1β content in the incubation medium. Similar data have been demonstrated in studies earlier [26, 27]. There was no increase of nuclear FITC-IgG number when macrophages were pre-incubated with selective PPARα antagonist GW6471 before LPS stimulation. This indicated that PPARα is not involved in the anti-inflammatory response after LPS treat compare to PPARγ, at least in the condition of our experiment. The NSE administration before treatment with LPS inhibited the LPS-mediated NF-kB translocation. Administration of PPARγ selective antagonist – GW 9662 resulted in intensification of NF-kB translocation and increased level of IL-1β in the medium. The correlation between inhibition of PPARγ and increased transcriptional activity of NF-κB has been previously well described [28]. The NSE administration after GW 9662 treatment and before LPS stimulation did not prevent the LPS-induced increase in the number of FITC-IgG particles in the nuclei of peritoneal macrophages. Therefore, NSE did not affect the NF-kB translocation during PPARγ inhibition caused by selective antagonist binding. However, when NSE was added before GW 9662 and LPS treatment, the level of NF-kB translocation and IL-1β content reduced to control cells' values. These data indicated a competitive binding of NSE with GW 9662 for the ligand-binding domen of PPARγ. It is worth to note that NSE administration to control cells did not affect the content of FITC-IgG particles in the nuclei of peritoneal macrophages.

The role of PPARs in the expression of genes that are involved in lipid metabolism, inflammation control, cell differentiation and various metabolic processes, especially lipid and glucose homeostasis is well established [29]. Moreover, the FATP1 and IL1RN are belong to PPARγ-target genes [30, 31]. In our study, we

found that NSE administration to obesity-induced IR rats significantly enhanced the liver expression of FATP1 and IL1-ra. These data indicated the possible interaction of NSE with PPARγ that resulted in the increase of FATP1 and IL1-ra mRNA expression. It is important to note that NSE administration to control rats, without obesity, did not cause any changes in FATP1 mRNA level, whereas decreased IL1ra mRNA level. As was shown in prior studies, only high concentrations of PPAR ligands triggered anti-inflammatory action by inhibiting the secretion of interleukin-1 (IL-1), interleukin-6 (IL-6) and tumor necrosis factor in stimulated monocytes [32]. Additionally reported that endogenous concentrations of N-acylethanolamides are normally at a very low rate (10^{-9} M), but their level dramatically increases in cases of pathological conditions [33]. We can suggest that exogenous administration of NSE to IR rats mediated the increase in its endogenous level that is required for PPARγ activation. However, further studies should be done in order to confirm this hypothesis.

Conclusion

In conclusion, our results demonstrated that PPARγ is involved in the anti-inflammatory action of NSE. The mechanism of NSE's action was mediated via activation of PPAR-γ and as a result suppressed nuclear translocation of NF-κB in peritoneal macrophages stimulated by LPS. The administration of NSE to IR rats changed the mRNA expression of several PPARγ - target gens. Thus, obtained findings suggested a promising therapeutic potential of NSE.

Declarations

Acknowledgements

Availability of Data and Material

The data used to support the findings of this study are available from the corresponding author upon request.

Code Availability

Not applicable.

Author information

Contributions

Kosiakova H., Berdyshev A., Herasymenko O., Dosenko V., Drevytska T. performed animal and laboratory experimens. Berdyshev A. and Dosenko V. contributed to data analysis and interpretation. Kosiakova H. wrote a draft of the manuscript. Kosiakova H. and Berdyshev A. contributed to the concept and design of the study. Hula N. coordinated the experiments and critically reviewed the manuscript.

Corresponding author

Correspondence to Halyna Kosiakova

Ethics declarations

Ethics Approval

The experimental procedures were approved by the Commission on Bioethics of Institute of Biochemistry, National Academy of Science, according with “General ethics principles on experiments with animals” of the 1st National Congress on Bioethics (Kyiv, 2001).

Consent to Participate

Not applicable.

Consent for Publication

Not applicable.

Competing Interests

The authors declare no competing interests.

Funding

This research was fully financed by National Academy of Science of Ukraine.

Conflicts of Interest

The authors declare no conflict of interest.

References

1. Gugliandolo, E., Peritore, A. F., Piras, C., Cuzzocrea, S., & Crupi, R. 2020. Palmitoylethanolamide and Related ALIAmides: Prohomeostatic Lipid Compounds for Animal Health and Wellbeing. Veterinary sciences, 7(2), 78. https://doi.org/10.3390/vetsci7020078.

2. Di Marzo V. 2008. Endocannabinoids: synthesis and degradation. Reviews of physiology, biochemistry and pharmacology, 160, 1–24. https://doi.org/10.1007/112_0505.

3. Di Marzo, V., Bisogno, T., De Petrocellis, L., Melck, D., & Martin, B. R. 1999. Cannabimimetic fatty acid derivatives: the anandamide family and other endocannabinoids. Current medicinal chemistry, 6(8), 721–744.

4. Gulaya, N. M., Kuzmenko, A. I., Margitich, V. M., Govseeva, N. M., Melnichuk, S. D., Goridko, T. M., & Zhukov, A. D. 1998. Long-chain N-acylethanolamides inhibit lipid peroxidation in rat liver mitochondria

under acute hypoxic hypoxia. Chemistry and physics of lipids, 97(1), 49–54. https://doi.org/10.1016/s0009-3084(98)00093-0.

5. Artamonov, M. V., Zhukov, O. D., Horid'ko, T. M., Klimashevs'kyĭ, V. M., Martseniuk, O. P., & Hula, N. M. 2003. Vplyv N-stearoïletanolaminu na lipidni komponenty mikrosom pechinky ta sertsia za diï na shchuriv ionizuiuchoho vyprominiuvannia [Effect of N-stearoylethanolamide and ionizing radiation on lipid components of the liver and heart microsomes in rats]. Ukrains'kyi biokhimichnyi zhurnal (1999), 75(4), 81–90.

6. Lykhmus, O., Kalashnyk, O., Uspenska, K., Horid'ko, T., Kosyakova, H., Komisarenko, S., & Skok, M. 2020. Different Effects of Nicotine and N-Stearoyl-ethanolamide on Episodic Memory and Brain Mitochondria of α7 Nicotinic Acetylcholine Receptor Knockout Mice. Biomolecules, 10(2), 226. https://doi.org/10.3390/biom10020226.

7. Artamonov, M., Zhukov, O., Shuba, I., Storozhuk, L., Khmel, T., Klimashevsky, V., Mikosha, A., & Gula, N. 2005. Incorporation of labelled N-acylethanolamide (NAE) into rat brain regions in vivo and adaptive properties of saturated NAE under x-ray irradiation. Ukrains'kyi biokhimichnyi zhurnal (1999), 77(6), 51–62.

8. Terrazzino, S., Berto, F., Dalle Carbonare, M., Fabris, M., Guiotto, A., Bernardini, D., & Leon, A. 2004. Stearoylethanolamide exerts anorexic effects in mice via down-regulation of liver stearoyl-coenzyme A desaturase-1 mRNA expression. FASEB journal : official publication of the Federation of American Societies for Experimental Biology, 18(13), 1580–1582. https://doi.org/10.1096/fj.03-1080fje.

9. Hula, N. M., Chumak, A. A., Berdyshev, A. H., Mehed', O. F., Horid'ko, T. M., Kindruk, N. L., Kosiakova, H. V., & Zhukov, O. D. 2009. Ukrains'kyi biokhimichnyi zhurnal (1999), 81(2), 107–116.

10. Onopchenko, O. V., Kosiakova, G. V., Klimashevsky, V. M., & Hula, N. M. 2015. The effect of N-stearoylethanolamide on plasma lipid composition in rats with experimental insulin resistance. Ukrainian biochemical journal, 87(1), 46–54.

11. Baldwin A. S., Jr. 2001. Series introduction: the transcription factor NF-kappaB and human disease. The Journal of clinical investigation, 107(1), 3–6. https://doi.org/10.1172/JCI11891.

12. Cheah, F. C., Hampton, M. B., Darlow, B. A., Winterbourn, C. C., & Vissers, M. C. 2005. Detection of apoptosis by caspase-3 activation in tracheal aspirate neutrophils from premature infants: relationship with NF-kappaB activation. Journal of leukocyte biology, 77(3), 432–437. https://doi.org/10.1189/jlb.0904520.

13. Cowburn, A. S., Deighton, J., Walmsley, S. R., & Chilvers, E. R. 2004. The survival effect of TNF-alpha in human neutrophils is mediated via NF-kappa B-dependent IL-8 release. European journal of immunology, 34(6), 1733–1743. https://doi.org/10.1002/eji.200425091.

14. Siednienko, J., & Gorczyca, W. A. 2003. Regulacja aktywności NF-kappa B [Regulation of NF-kappa B activity]. Postepy higieny i medycyny doswiadczalnej, 57(1), 19–32.

15. Berdyshev, A. G., Kosiakova, H. V., Onopchenko, O. V., Panchuk, R. R., Stoika, R. S., & Hula, N. M. 2015. N-Stearoylethanolamide suppresses the pro-inflammatory cytokines production by inhibition of NF-κB translocation. Prostaglandins & other lipid mediators, 121(Pt A), 91–96. https://doi.org/10.1016/j.prostaglandins.2015.05.001.

16. Scirpo, R., Fiorotto, R., Villani, A., Amenduni, M., Spirli, C., & Strazzabosco, M. 2015. Stimulation of nuclear receptor peroxisome proliferator-activated receptor-γ limits NF-κB-dependent inflammation in mouse cystic fibrosis biliary epithelium. Hepatology (Baltimore, Md.), 62(5), 1551–1562. https://doi.org/10.1002/hep.28000.

17. Ruan, H., Pownall, H. J., & Lodish, H. F. 2003. Troglitazone antagonizes tumor necrosis factor-alpha-induced reprogramming of adipocyte gene expression by inhibiting the transcriptional regulatory functions of NF-kappaB. The Journal of biological chemistry, 278(30), 28181–28192. https://doi.org/10.1074/jbc.M303141200

18. Hula, N. M., Chumak, A. A., Mehed', O. F., Horid'ko, T. M., Kindruk, N. L., & Berdyshev, A. H. 2008. Ukrains'kyi biokhimichnyi zhurnal (1999), 80(1), 57–67.

19 [1]. Lykhmus, O., Uspenska, K., Koval, L., Lytovchenko, D., Voytenko, L., Horid'ko, T., Kosiakova, H., Gula, N., Komisarenko, S., & Skok, M. 2017. N-Stearoylethanolamide protects the brain and improves memory of mice treated with lipopolysaccharide or immunized with the extracellular domain of α7 nicotinic acetylcholine receptor. International immunopharmacology, 52, 290–296. https://doi.org/10.1016/j.intimp.2017.09.023.

20. Epps, D. E., Natarajan, V., Schmid, P. C., & Schmid, H. O. 1980. Accumulation of N-acylethanolamide glycerophospholipids in infarcted myocardium. Biochimica et biophysica acta, 618(3), 420–430. https://doi.org/10.1016/0005-2760(80)90260-x.

21. Sancho, R., Calzado, M. A., Di Marzo, V., Appendino, G., & Muñoz, E. 2003. Anandamide inhibits nuclear factor-kappaB activation through a cannabinoid receptor-independent pathway. Molecular pharmacology, 63(2), 429–438. https://doi.org/10.1124/mol.63.2.429.

22. Peritore, A. F., Siracusa, R., Crupi, R., & Cuzzocrea, S. 2019. Therapeutic Efficacy of Palmitoylethanolamide and Its New Formulations in Synergy with Different Antioxidant Molecules Present in Diets. Nutrients, 11(9), 2175. https://doi.org/10.3390/nu11092175.

23. Berdyshev A.G., Kosiakova H.V., Hula N.M. 2017. Modulation of LPS-induced ROS production and NF-κB nuclear translocation by N-stearoylethanolamide in macrophages. Ukrains'kyi biokhimichnyi zhurnal (1999), 89(5), 62–69.

24. Heming, M., Gran, S., Jauch, S. L., Fischer-Riepe, L., Russo, A., Klotz, L., Hermann, S., Schäfers, M., Roth, J., & Barczyk-Kahlert, K. 2018. Peroxisome Proliferator-Activated Receptor-γ Modulates the Response of Macrophages to Lipopolysaccharide and Glucocorticoids. Frontiers in immunology, 9, 893. https://doi.org/10.3389/fimmu.2018.00893.

25. Wang, J., Xiao, C., Wei, Z., Wang, Y., Zhang, X., & Fu, Y. 2018. Activation of liver X receptors inhibit LPS-induced inflammatory response in primary bovine mammary epithelial cells. Veterinary immunology and immunopathology, 197, 87–92. https://doi.org/10.1016/j.vetimm.2018.02.002.

26. Scirpo, R., Fiorotto, R., Villani, A., Amenduni, M., Spirli, C., & Strazzabosco, M. 2015. Stimulation of nuclear receptor peroxisome proliferator-activated receptor-γ limits NF-κB-dependent inflammation in mouse cystic fibrosis biliary epithelium. Hepatology (Baltimore, Md.), 62(5), 1551–1562. https://doi.org/10.1002/hep.28000.

27. Scirpo, R., Fiorotto, R., Villani, A., Amenduni, M., Spirli, C., & Strazzabosco, M. 2015. Stimulation of nuclear receptor peroxisome proliferator-activated receptor-γ limits NF-κB-dependent inflammation in mouse cystic fibrosis biliary epithelium. Hepatology (Baltimore, Md.), 62(5), 1551–1562. https://doi.org/10.1002/hep.28000.

28. Nakanishi, A., & Tsukamoto, I. 2015. n-3 polyunsaturated fatty acids stimulate osteoclastogenesis through PPARγ-mediated enhancement of c-Fos expression, and suppress osteoclastogenesis through PPARγ-dependent inhibition of NFkB activation. The Journal of nutritional biochemistry, 26(11), 1317–1327. https://doi.org/10.1016/j.jnutbio.2015.06.007.

29. Grygiel-Górniak B. 2014. Peroxisome proliferator-activated receptors and their ligands: nutritional and clinical implications–a review. Nutrition journal, 13, 17. https://doi.org/10.1186/1475-2891-13-17.

30. Shysh, A. M., Nagibin, V. S., Kaplinskii, S. P., & Dosenko, V. E. 2016. N-3 long chain polyunsaturated fatty acids increase the expression of PPARγ-target genes and resistance of isolated heart and cultured cardiomyocytes to ischemic injury. Pharmacological reports : PR, 68(6), 1133–1139. https://doi.org/10.1016/j.pharep.2016.06.013.

31. Martin, G., Schoonjans, K., Lefebvre, A. M., Staels, B., & Auwerx, J. 1997. Coordinate regulation of the expression of the fatty acid transport protein and acyl-CoA synthetase genes by PPARalpha and PPARgamma activators. The Journal of biological chemistry, 272(45), 28210–28217. https://doi.org/10.1074/jbc.272.45.28210.

32. Meier, C. A., Chicheportiche, R., Juge-Aubry, C. E., Dreyer, M. G., & Dayer, J. M. 2002. Regulation of the interleukin-1 receptor antagonist in THP-1 cells by ligands of the peroxisome proliferator-activated receptor gamma. Cytokine, 18(6), 320–328. https://doi.org/10.1006/cyto.2002.1945.

33. Balvers, M. G., Verhoeckx, K. C., Meijerink, J., Wortelboer, H. M., & Witkamp, R. F. 2013. Measurement of palmitoylethanolamide and other N-acylethanolamides during physiological and pathological conditions.

CNS & neurological disorders drug targets, 12(1), 23–33.
https://doi.org/10.2174/1871527311312010007.

Figures

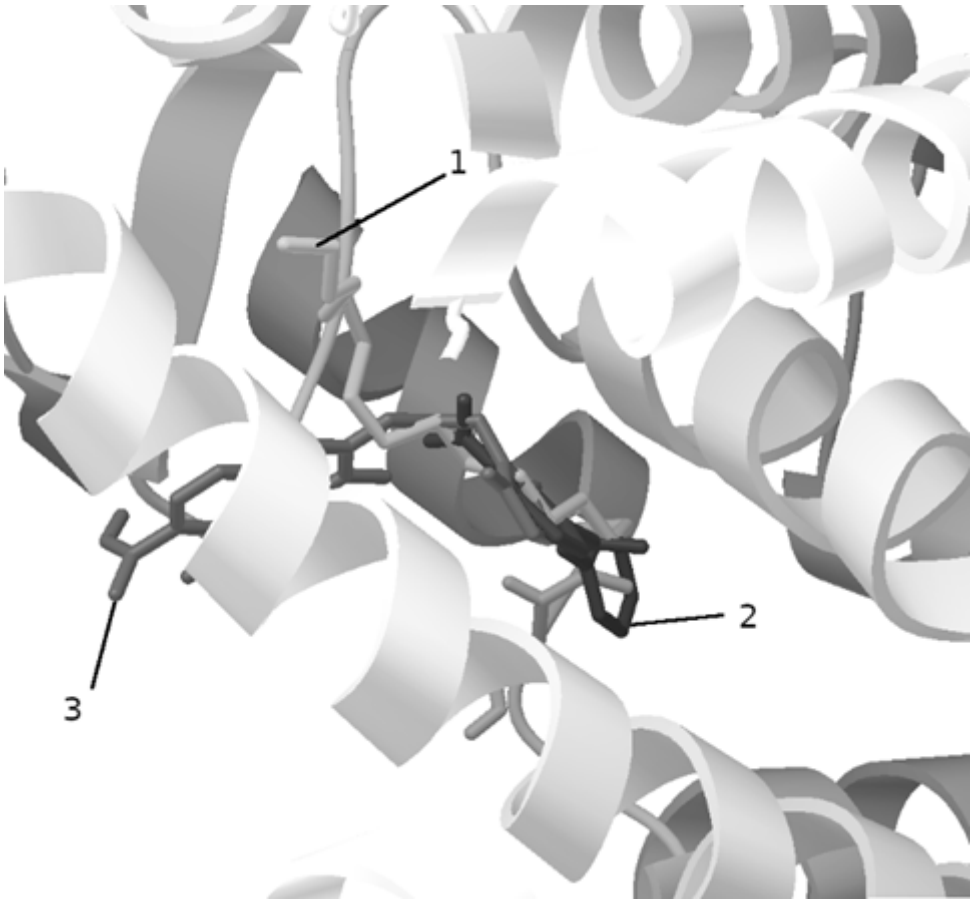

Figure 1

Results of independent NSE, GW6992 and LY171883 docking in the PPARγ ligand binding domain (3b0r). 1 – NSE. 2 – GW9662. 3 – LY171883

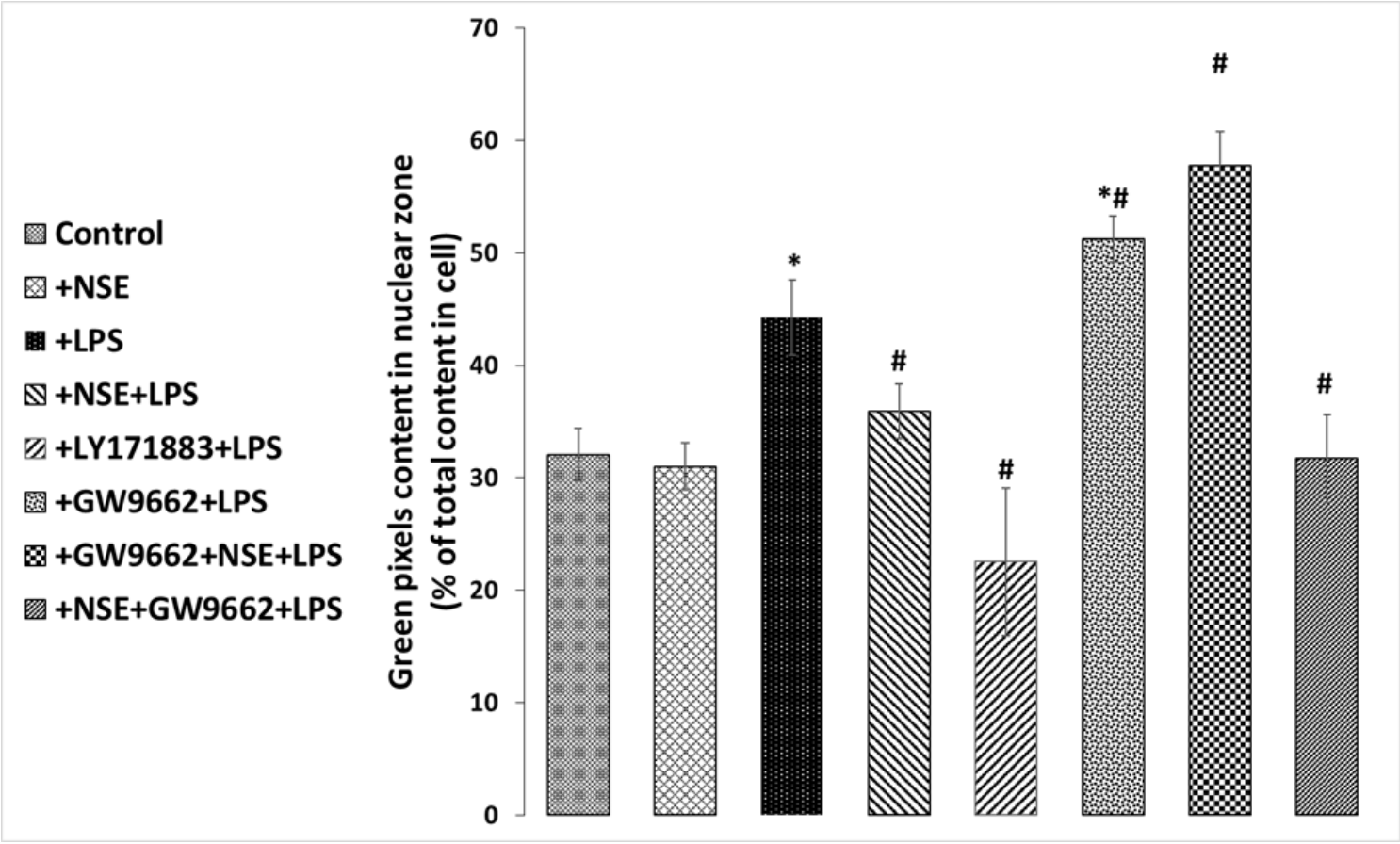

Figure 2

The number of FITC-IgG particles in the nuclei of the peritoneal macrophages of normal rats. Values are presented as mean ± SEM (n=8-42). * - P<0,05 compare to the control macrophages; # - P<0,05 compare to the LPS-activated macrophages.

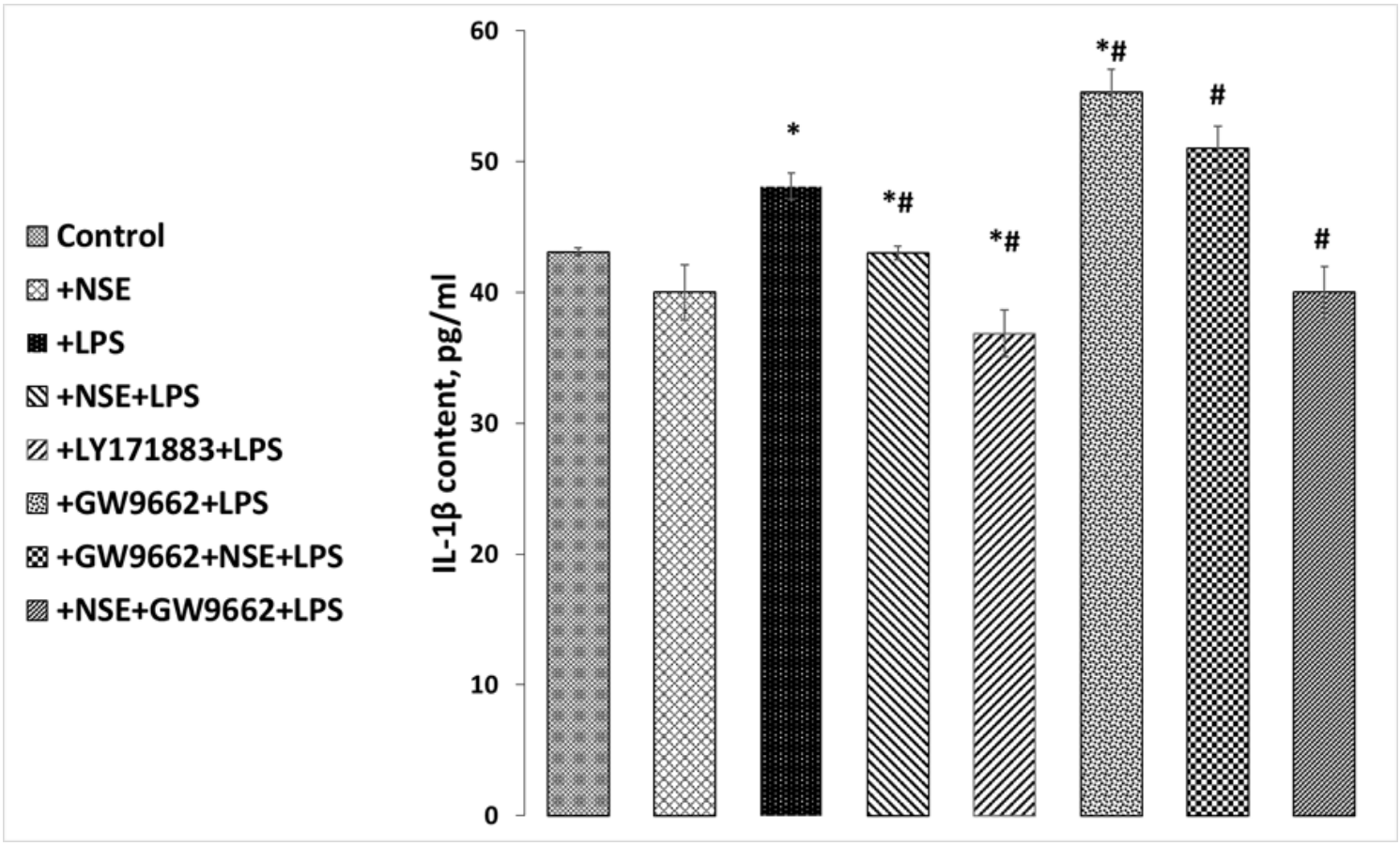

Figure 3

The IL-1β content in the culture supernatant.

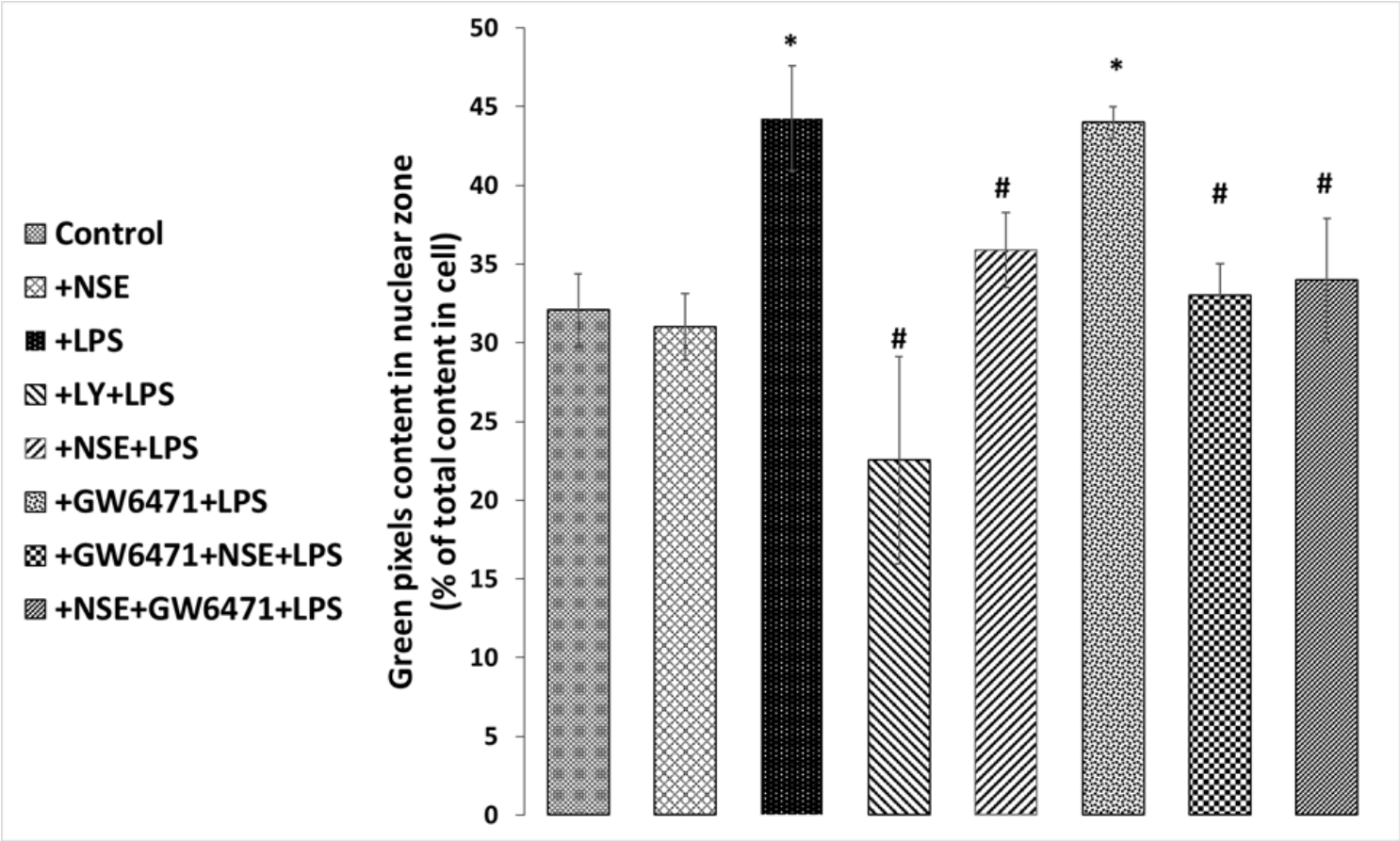

Figure 4

The number of FITC-IgG particles in the nuclei of peritoneal macrophages from control rats. Values are presented as mean ± SEM (n=8-42) * - P<0,05 compare to control macrophages; # - P<0,05 compare to LPS-activated macrophages.

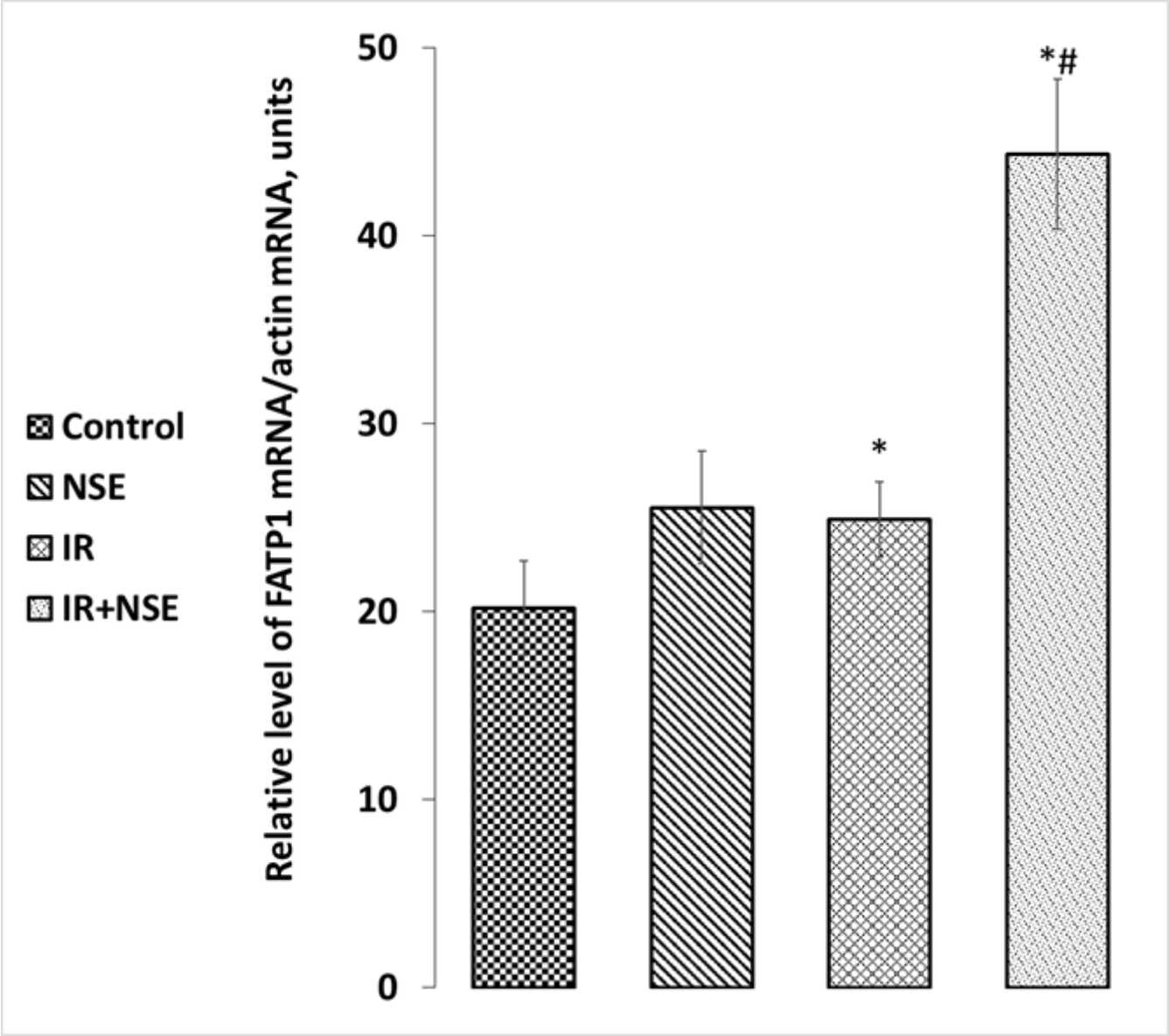

Figure 5

Relative level of mRNA FATP1expression in rat liver.

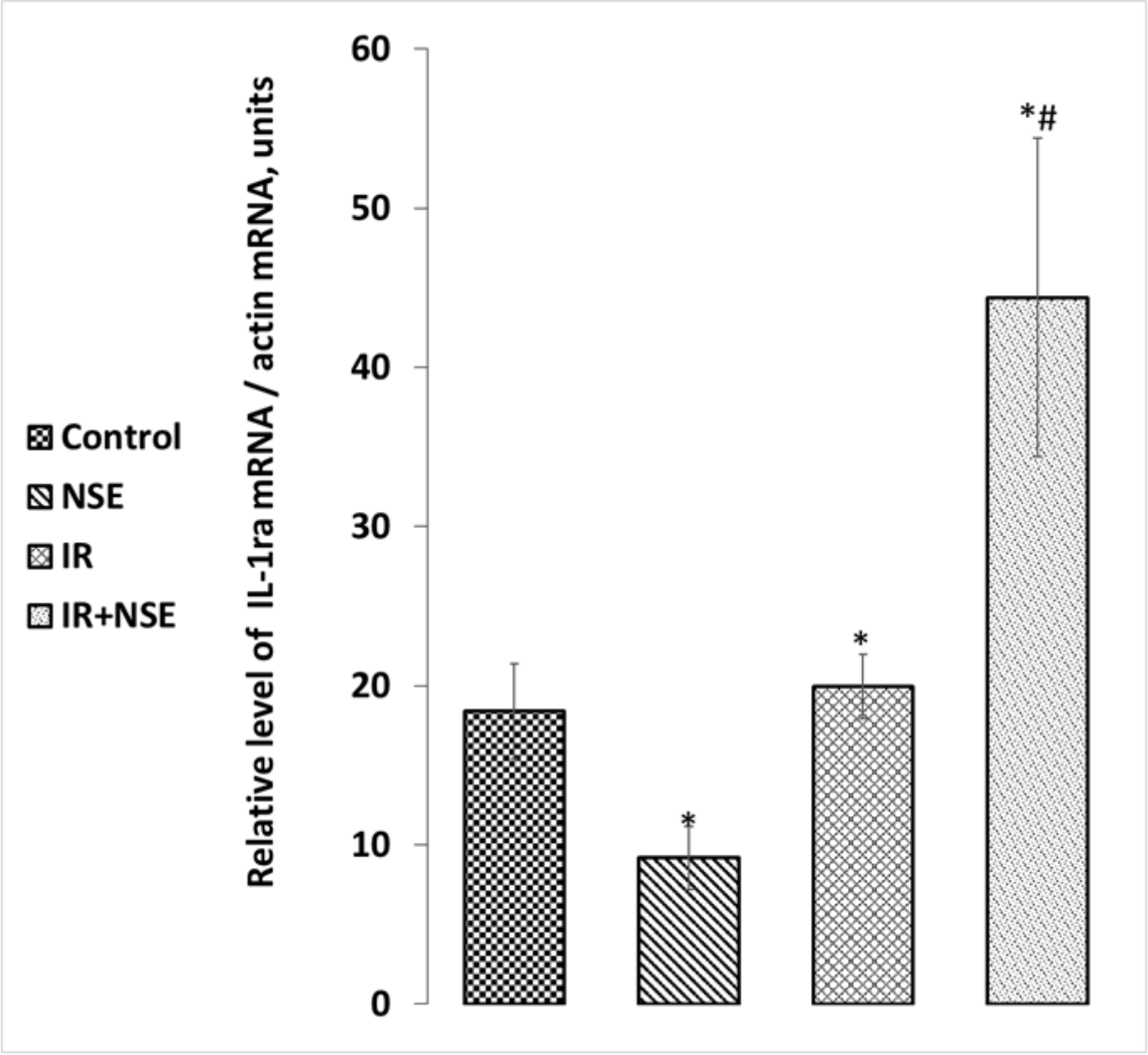

Figure 6

Relative level of mRNA IL1ra expression in rat liver.

Supplementary Files

This is a list of supplementary files associated with this preprint. Click to download.

- SupplementaryInformation.pdf